



Measurements of supersonic boundary layer turbulence with a dynamic pitot probe
by Terrance Gerard Tritz

A thesis submitted in partial fulfillment of the requirements for the degree of Master of Science in
Mechanical Engineering
Montana State University
© Copyright by Terrance Gerard Tritz (1990)

Abstract:

The use of a dynamic pitot probe to measure fluctuating pitot pressure of supersonic flow was investigated. Data were taken at three wind tunnel positions and 20 $Re\theta$ values. Mean flow measurements were taken to characterize the flow. The mean flow data were found to be consistent with previous data taken in the wind tunnel. An $Re\theta$ effect was also found. The flow appeared to have been in the transition region based on the mean flow measurements and a law of the wall analysis. Wideband RMS velocity measurements were obtained from the fluctuating pressure measurements with the dynamic pitot probe. An $Re\theta$ effect was also found for the wideband RMS data. The wideband measurements also supported the conclusion of transitional flow drawn from the mean flow data. Intermittency measurements of the boundary layer showed that the boundary layer thickness could differ depending on whether a time-average method or an intermittency method is used to define the edge of the boundary layer. Spectral measurements were made at the highest $Re\theta$ value of 2073. The dissipation spectra, in general, agreed with Pao's theory with much less scatter than previously experienced. The dissipation function was able to be measured precisely compared to previous methods which were unacceptable due to scatter. The velocity spectra approached the universal spectrum in a way dependent on the distance from the tunnel wall. Accurate measurement of signals at frequencies greater than 1 Megahertz in the boundary layer were obtained.

**MEASUREMENTS OF SUPERSONIC BOUNDARY LAYER
TURBULENCE WITH A DYNAMIC PITOT PROBE**

by

Terrance Gerard Tritz

A thesis submitted in partial fulfillment
of the requirements for the degree

of

Master of Science

in

Mechanical Engineering

MONTANA STATE UNIVERSITY
Bozeman, Montana

May 1990

1378
T9395

APPROVAL

of a thesis submitted by

Terrance Gerard Tritz

This thesis has been read by each member of the thesis committee and has been found to be satisfactory regarding content, English usage, format, citations, bibliographic style, and consistency, and is ready for submission to the College of Graduate Studies.

5/18/90
Date

A. K. Smith
Chairperson, Graduate Committee

Approved for the Major Department

5/18/90
Date

N. E. Larsen
Head, Major Department

Approved for the College of Graduate Studies

May 24, 1990
Date

Henry L. Parsons
Graduate Dean

STATEMENT OF PERMISSION TO USE

In presenting this thesis in partial fulfillment of the requirements for a master's degree at Montana State University, I agree that the Library shall make it available to borrowers under rules of the Library. Brief quotations from this thesis are allowable without special permission, provided that accurate acknowledgment of source is made.

Permission for extensive quotation from or reproduction of this thesis may be granted by my major professor, or in his absence, by the Dean of Libraries when, in the opinion of either, the proposed use of the material is for scholarly purposes. Any copying or use of the material in this thesis for financial gain shall not be allowed without my written permission.

Signature Terrence A. Tubz

Date 5-18-90

ACKNOWLEDGMENTS

The author is indebted to the following persons for their contributions to this investigation:

His advisor, Dr. Anthony Demetriades, for his guidance throughout the investigation.

John Rompel, for designing and constructing the special electronic equipment used in the investigation.

Pat Vowell, for his assistance in constructing the equipment used in the investigation.

Dr. William Martindale, Dr. Thomas Reihman and Dr. Robert Boik for their support as committee members.

The Department of Mechanical Engineering for financial assistance.

Both sets of parents, who always gave support and encouragement.

Special thanks to his wife, Rene', for typing the thesis and for her encouragement and understanding during this graduate program.

TABLE OF CONTENTS

	<u>Page</u>
LIST OF TABLES	vii
LIST OF FIGURES	viii
NOMENCLATURE	xii
ABSTRACT	xiv
1. INTRODUCTION	1
2. EXPERIMENTAL SETUP	5
Facilities	5
Wind Tunnel	5
Flow Conditions	6
Mean Flow Setup	6
Pitot Tube	6
Data Acquisition System	8
Dynamic Pitot Probe Setups	8
Dynamic Pitot Probe	8
Data Acquisition Systems	11
3. EXPERIMENTAL RESULTS	17
Mean Flow Measurements	17
Introduction	17
Mean Flow Data Reduction	17
Mean Flow Results	19
Law of the Wall Analysis	21
Coefficient of Friction	22
Wideband RMS Measurements	24
Data Reduction	24
Wideband RMS Results	24
Intermittency Measurements	26
Introduction	26
Results	28

TABLE OF CONTENTS—Continued

	<u>Page</u>
3. EXPERIMENTAL RESULTS (continued)	
Power Spectrum Measurements	31
Introduction	31
Fast Fourier Transform Data Reduction	31
Universal Spectrum Data Reduction	36
Universal Spectrum Results	45
4. CONCLUSIONS	62
Mean Flow	62
Wideband Measurements	62
Spectral Analysis	63
REFERENCES CITED	64
APPENDICES	67
Appendix A – Boundary Layer Data Conversion Program	68
Appendix B – Law of the Wall Program	77
Appendix C – Spectral Analysis Program	80
Appendix D – Noise Removal and Integrand Calculation Program	85
Appendix E – Spectral Non-Dimensionalization Program	87

LIST OF TABLES

Table	<u>Page</u>
1. Comparison of FFT Measurements with RMS Meter	35

LIST OF FIGURES

Figure	<u>Page</u>
1. Test Section of MSU Supersonic Wind Tunnel	7
2. Major Features of the DPP	9
3. Electronic Circuit used with DPP	11
4. Oscilloscope Amplication	13
5. Setup of DPP Data Acquisition System	16
6. Boundary Layer Velocity Profiles	20
7. Velocity at the Midpoint of the Boundary Layer	20
8. Law of the Wall Profiles	23
9. Comparison of C_f with Turbulent Datum and Theory	23
10. Velocity RMS Fluctuation Levels	25
11. Velocity RMS Fluctuation Levels at $y/\delta = .5$	25
12. Typical Output from the Intermittency Meter	27
13. Comparison of Two Methods for Boundary Layer Thickness Measurement	29
14. Intermittency Level Dependence on y/δ	30
15. Comparison of Noise Measurements	34
16. RMS Voltage Spectrum at $y/\delta = .091$	39
17. Integrand of Dissipation Function at $y/\delta = .091$	39
18. RMS Voltage Spectrum at $y/\delta = .496$ (# 1)	40

LIST OF FIGURES—Continued

Figure	Page
19. Integrand of Dissipation Function at $y/\delta = .496$ (# 1)	40
20. RMS Voltage Spectrum at $y/\delta = .496$ (# 2)	41
21. Integrand of Dissipation Function at $y/\delta = .496$ (# 2)	41
22. RMS Voltage Spectrum at $y/\delta = .738$	42
23. Integrand of Dissipation Function at $y/\delta = .738$	42
24. RMS Voltage Spectrum at $y/\delta = .981$	43
25. Integrand of Dissipation Function at $y/\delta = .981$	43
26. RMS Voltage Spectrum in the Freestream	44
27. Integrand of Dissipation Function in the Freestream	44
28. Incompressible Spectra Compared to Universal Spectrum	48
29. Re_λ Comparison	48
30. Kolmogoroff Wave Number	49
31. Microscale Comparison	49
32. Dissipation Function Comparison	50
33. Wideband Velocity RMS Fluctuations	50
34. Non-Dimensional Spectrum at $y/\delta = .091$	51
35. Non-Dimensional Spectrum at $y/\delta = .131$	51
36. Non-Dimensional Spectrum at $y/\delta = .172$	52
37. Non-Dimensional Spectrum at $y/\delta = .212$	52

LIST OF FIGURES—Continued

Figure	<u>Page</u>
38. Non-Dimensional Spectrum at $y/\delta = .253$	53
39. Non-Dimensional Spectrum at $y/\delta = .293$	53
40. Non-Dimensional Spectrum at $y/\delta = .334$	54
41. Non-Dimensional Spectrum at $y/\delta = .374$	54
42. Non-Dimensional Spectrum at $y/\delta = .415$	55
43. Non-Dimensional Spectrum at $y/\delta = .445$	55
44. Non-Dimensional Spectrum at $y/\delta = .496$ (# 1)	56
45. Non-Dimensional Spectrum at $y/\delta = .496$ (# 2)	56
46. Non-Dimensional Spectrum at $y/\delta = .536$	57
47. Non-Dimensional Spectrum at $y/\delta = .576$	57
48. Non-Dimensional Spectrum at $y/\delta = .698$	58
49. Non-Dimensional Spectrum at $y/\delta = .738$	58
50. Non-Dimensional Spectrum at $y/\delta = .779$	59
51. Non-Dimensional Spectrum at $y/\delta = .860$	59
52. Non-Dimensional Spectrum at $y/\delta = .900$	60
53. Non-Dimensional Spectrum at $y/\delta = .981$	60
54. Comparison of Two Spectra taken at $y/\delta = .496$	61
55. Reynolds Number Dependence of the Velocity Spectrum at a Low Wavenumber	61
56. Boundary Layer Data Conversion Program	69

LIST OF FIGURES—Continued

Figure	<u>Page</u>
57. Law of the Wall Program	78
58. Spectral Analysis Program	81
59. Noise Removal and Integrand Calculation Program	86
60. Spectral Non-Dimensionalization Program	88

NOMENCLATURE

<i>a</i>	constant for law of the wall calculations
a.f.	amplification factor
<i>b</i>	constant for law of the wall calculations
C_f	coefficient of friction
d.c.	direct current
<i>f</i>	frequency
<i>H</i>	frequency dependent variable for Fourier transform
<i>h</i>	time dependent variable in Fourier transform
I_u	integral within the dissipation function
<i>i</i>	square root of -1
<i>k</i>	wavenumber
<i>M</i>	Mach number
<i>m</i>	variable used in Fourier Transform (value = 0 to $N - 1$)
<i>N</i>	number of points taken in each waveform
<i>n</i>	variable used for summation in Fourier Transforms
<i>P</i>	pressure
<i>R</i>	gas constant
<i>Re</i>	Reynolds number
RMS	root mean square
<i>s</i>	sensitivity coefficient
<i>T</i>	temperature

NOMENCLATURE—Continued

t	time
u	velocity
y	position from wall
δ	boundary layer thickness
δ_I	boundary layer thickness based on intermittency
ϵ	dissipation function
γ	specific heat ratio
λ	velocity microscale
ρ	density
θ	momentum thickness
ν	kinematic viscosity
ϕ	non-dimensional power spectrum
π	3.14159...
∞	infinity
$()_2$	condition after normal shock
$()_0$	isentropic stagnation property
$()_e$	boundary layer edge condition
$()_K$	Kolmogoroff property
$()_P$	stagnation property after normal shock
$()_w$	property at wall
$()^+$	law of the wall variable
$()'$	RMS quantity
$\overline{()}$	property transformed to the incompressible plane

ABSTRACT

The use of a dynamic pitot probe to measure fluctuating pitot pressure of supersonic flow was investigated. Data were taken at three wind tunnel positions and 20 Re_θ values. Mean flow measurements were taken to characterize the flow. The mean flow data were found to be consistent with previous data taken in the wind tunnel. An Re_θ effect was also found. The flow appeared to have been in the transition region based on the mean flow measurements and a law of the wall analysis. Wideband RMS velocity measurements were obtained from the fluctuating pressure measurements with the dynamic pitot probe. An Re_θ effect was also found for the wideband RMS data. The wideband measurements also supported the conclusion of transitional flow drawn from the mean flow data. Intermittency measurements of the boundary layer showed that the boundary layer thickness could differ depending on whether a time-average method or an intermittency method is used to define the edge of the boundary layer. Spectral measurements were made at the highest Re_θ value of 2073. The dissipation spectra, in general, agreed with Pao's theory with much less scatter than previously experienced. The dissipation function was able to be measured precisely compared to previous methods which were unacceptable due to scatter. The velocity spectra approached the universal spectrum in a way dependent on the distance from the tunnel wall. Accurate measurement of signals at frequencies greater than 1 Megahertz in the boundary layer were obtained.

CHAPTER 1

INTRODUCTION

Currently, more knowledge is needed to understand turbulent and transitional boundary layers in supersonic flows. Design of supersonic vehicles is one area that requires more information on the friction and heat transfer characteristics of turbulent and transitional flows.

Essential to the understanding of these flows are the wideband fluctuation levels which enter the equations of motion as unpredictable unknowns. Numerous studies have been made of low-speed wideband fluctuation levels in turbulent boundary layers but data are very scarce at high speeds. The effect of Mach number on fluctuation levels in the high-speed boundary layer was investigated by Laderman and Demetriades [1]. They studied data from several sources whose data covered the edge Mach number range 0 to 9.4 and was measured mainly with the use of hot-wire anemometers and found that there was a Mach number effect on the fluctuation levels.

Owen, et al [2] also studied the effect of unit Reynolds number ($\equiv u_e/\nu_e$) on fluctuation levels in transitional boundary layers at $M = 7$ using a film anemometer technique. They used the level of film voltage fluctuations to study qualitatively the transition "history" of the boundary layer.

Also important are the spectral characteristics of these boundary layers. Much work has been done on the velocity spectrum of low speed turbulent boundary layers, for example Pao [3] and Uberoi and Freymuth [4]. Demetriades and

Martindale [5], [6] have reported work on the supersonic and hypersonic turbulent boundary layer spectra with Mach numbers from 3 to 9.4, using hot-wire anemometers. They found that the non-dimensional power spectra followed low speed theory which included a Reynolds number dependence. Very little work has been done on the fluctuation spectra in supersonic transitional boundary layers.

The major difficulty of the wideband measurements is that none of the work has determined if there is any systematic Re_θ effect. The data in [1] did show a Mach number effect but does not investigate the effect of Re_θ . To generalize to any boundary layer a Re_θ dependence needs to be found.

Reference [2] presented the evolution of fluctuations in the transition zone. This work did not involve any investigation of an Re_θ effect. It also did not involve any quantitative measurement of velocity fluctuations or power spectra. Instead it used the film voltage fluctuations only to show where the transition region occurred. Therefore very little quantitative knowledge of the wideband fluctuations exists in the transition region.

The hot-wire anemometer, which is used for most velocity fluctuation measurements, has several difficulties. First, in all cases the hot-wire frequency response limitations require complicated mathematical corrections to the hot-wire signals. This affects both the wideband and frequency-dependent measurements through the introduction of errors.

Second, due to the frequency limitations mentioned and the noise of the system required to measure the hot-wire signals, the highest frequency signal capable of being accurately measured by a hot-wire anemometer is approximately 600 kilohertz according to [1]. This limit on frequency also affects the dissipation spectra. Due to noise problems, [1] reported severe difficulties in measuring the spectrum at high frequencies. In the same reference the dissipation spectrum, needed to

express the spectrum in universal form, was shown to be almost impossible to measure with the hot-wire anemometer at high speeds. In fact, in [5] and [6] there were several dissipation spectra which did not return to zero, as they should at high frequencies. In this case the dissipation function, which is the integral of the dissipation spectrum, could not be computed from the data without major assumptions.

The third problem in high-speed flows is that the hot-wire anemometer is extremely fragile. This can cause long delays in experiments and require that several hot-wire anemometers are calibrated in advance of any experiment.

A dynamic pitot probe was chosen here as the best probe to eliminate the disadvantages of the hot-wire anemometer. Not only was this dynamic pitot probe durable but its frequency range extended to at least 1.5 Megahertz. This frequency range enabled measurement at frequencies much higher than would have been possible with the hot-wire anemometer. Because this probe had such good frequency response, no complex mathematical corrections were needed to measure spectra at high frequencies.

With the dynamic pitot probe, the goal was to make fluctuation measurements and compare the measurements with past data where possible. Since a new probe was involved its readings must be consistent with previous turbulence data. Mean flow data taken at the same time in the transition zone should also be consistent with the mean flow measured previously in the fully turbulent boundary layer. With such measurements, characterization of the transitional supersonic boundary layer and its turbulence is possible including a Re_θ effect.

In addition to characterizing the supersonic boundary layer in general, the dynamic pitot probe had unique promise in measuring the high frequency turbulence components. This ability raised the possibility of obtaining dissipation spectra and

dissipation functions accurately for the first time ever in high-speed flows. With this possibility, the development of the transition zone non-dimensional spectra and their relation to the universal turbulent spectrum could be observed.

CHAPTER 2

EXPERIMENTAL SETUP

Facilities

Wind Tunnel

All of the experimental work was performed in the Montana State University Wind Tunnel (SWT). The SWT uses air as the working fluid and has a nominal Mach number of 3 in the test section. The unit Reynolds number ranges from 48,000 to 140,000 per inch. For a more detailed description of this facility refer to Drummond et al [7].

In order to achieve the goals mentioned in Chapter 1, the regions in the wind tunnel with transitional or turbulent boundary layers had to be found. References [7] and [8] showed that stagnation pressures between 300 and 400 torr would cause the onset of transition in the floor boundary layer of the wind tunnel test section. The further downstream the measurements were made, the lower the stagnation pressure needed for a transitional boundary layer.

Based on this information, the region chosen for measurement of the boundary layer was the farthest downstream position in the wind tunnel test section within the range of movement of the dynamic pitot probe.

In order to achieve as wide a range of Re_θ ($\equiv \frac{u_e \theta}{\nu_e}$) as possible, three positions in the test section were chosen for boundary layer measurements. Also

approximately seven stagnation pressures were chosen to help vary Re_θ . The total number of pressures at any position depended on the wind tunnel's ability to maintain supersonic flow. Since the combination of positions and total pressures would give 21 Re_θ 's only one total temperature was used.

Flow Conditions

The three positions of the SWT floor chosen for boundary layer measurements were $x = .4, 1.6$ and 2.9 inches as measured from the front of the extension block seen in Figure 1 reproduced from [7] which shows the test section of the SWT. The free stream total temperature was maintained at a nominal 100 degrees Fahrenheit and the free stream total pressure was varied from 600 to 430 torr in increments of 20 or 30 torr. The total temperature and pressure were recorded for later use in data reduction. The range of Re_θ was 1016 to 2073 for these conditions.

Mean Flow Setup

Pitot Tube

A .005 inch pitot tube was used to make the mean flow measurements in the boundary layer. The time-average streamwise velocity (u), local Mach number and local static temperature were the main characteristics measured. A Kulite XTH-1-190-5A pressure transducer was inside the pitot tube housing and converted the pitot pressure to a d.c. voltage. The smallest boundary layer thickness measured was .146 inches based on 99 percent of the edge velocity. This gave a minimum resolution, based on the ratio of the pitot tube diameter to the thinnest boundary layer, for the pitot tube of .034.

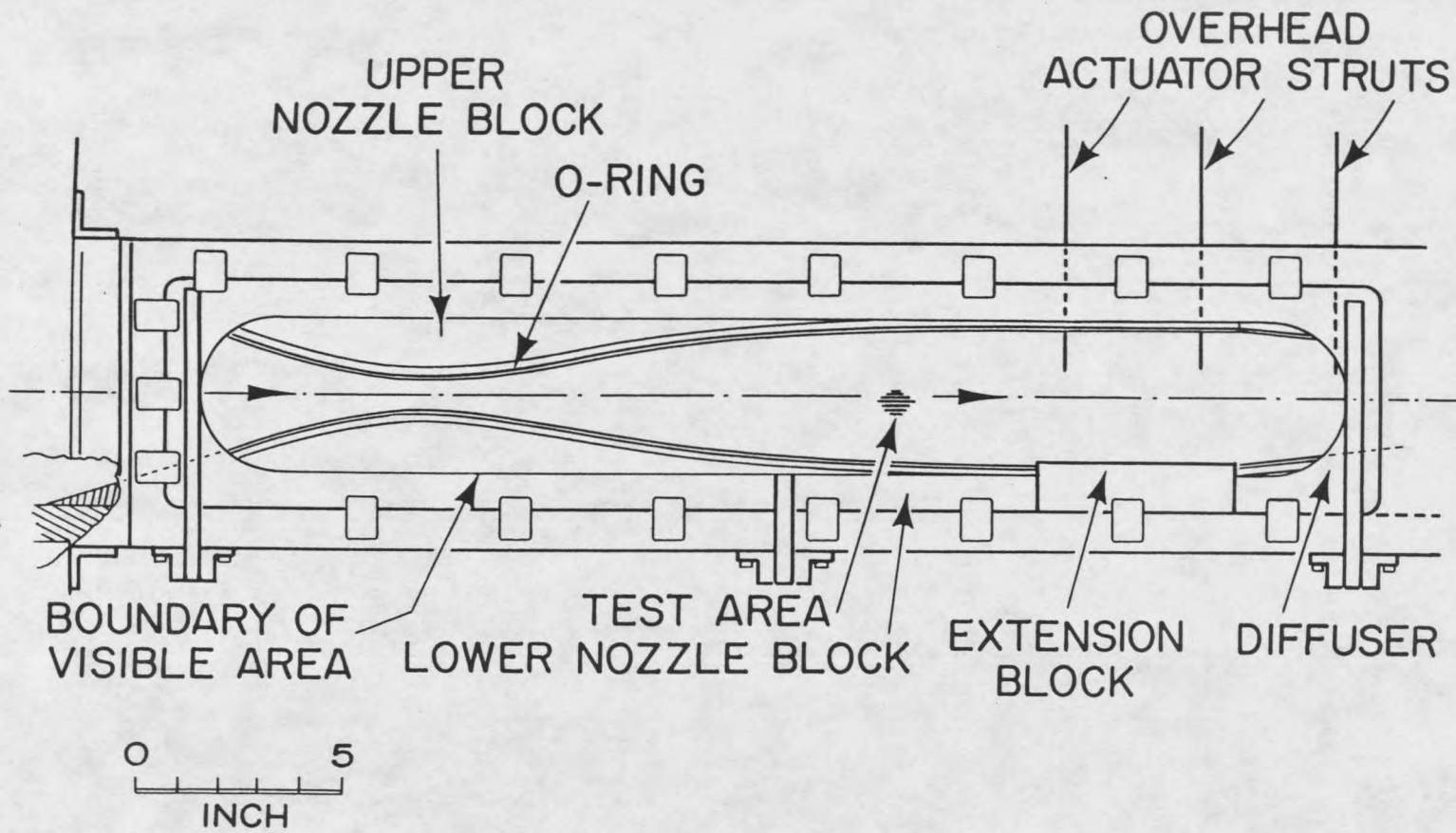


Figure 1. Test Section of MSU Supersonic Wind Tunnel.

Data Acquisition System

All mean flow data were taken using the SWT Automated Data Acquisition System. This system employed a Zenith Z-100 computer with an analog to digital card for conversion of the analog voltage from the pitot transducer to a digital reading. The first reading was taken at .0225 inches from the floor of the tunnel, since this distance was the closest that the probe used for fluctuation measurements could approach the floor. Subsequent readings were taken every .005 inches until the probe was .5 inches from the floor. All mean flow data were recorded directly on disk for storage and data reduction. For further information on the mean flow data acquisition system refer to Berger [9].

Dynamic Pitot Probe Setups

Dynamic Pitot Probe

A dynamic pitot probe (DPP) was used for all fluctuation flow measurements. The DPP, model CQ-030-100G, is a differential pressure transducer using a four arm Wheatstone bridge in a silicon diaphragm for sensing built by Kulite Semiconductor Products, Inc. The DPP has an outside diameter of .032 inches and an active area diameter of .010 inches, giving it a minimum resolution, based on the ratio of active area diameter to thinnest boundary layer thickness, of .068. The natural frequency of the DPP is 1.5 Megahertz. The DPP was used for fluctuating measurements only as it is incapable of mean flow measurements.

Since the DPP is a differential pressure transducer, it included a reference tube which could be connected to a pressure source. Since this pressure was unnecessary for fluctuating pressure measurements, the reference tube was left open to atmospheric pressure.

The sensitivity of the DPP is given by Kulite as .0982 millivolts/pounds per square inch/volts d.c. (from the power supply). From previous experimentation it was determined, using a mean flow calibration method, that the calculated sensitivities came within 17 percent of Kulite's stated sensitivity. It was then decided (Demetriades [10]) to accept Kulite's calibration since the DPP cannot measure mean flow conditions. Therefore the DPP cannot be accurately calibrated with the mean flow method employed.

The DPP was housed at the end of a fin attached to a sting. As can be seen in Figure 2, reproduced from [8], this arrangement allowed the DPP to take measurements near the floor of the tunnel as was needed for this experiment.

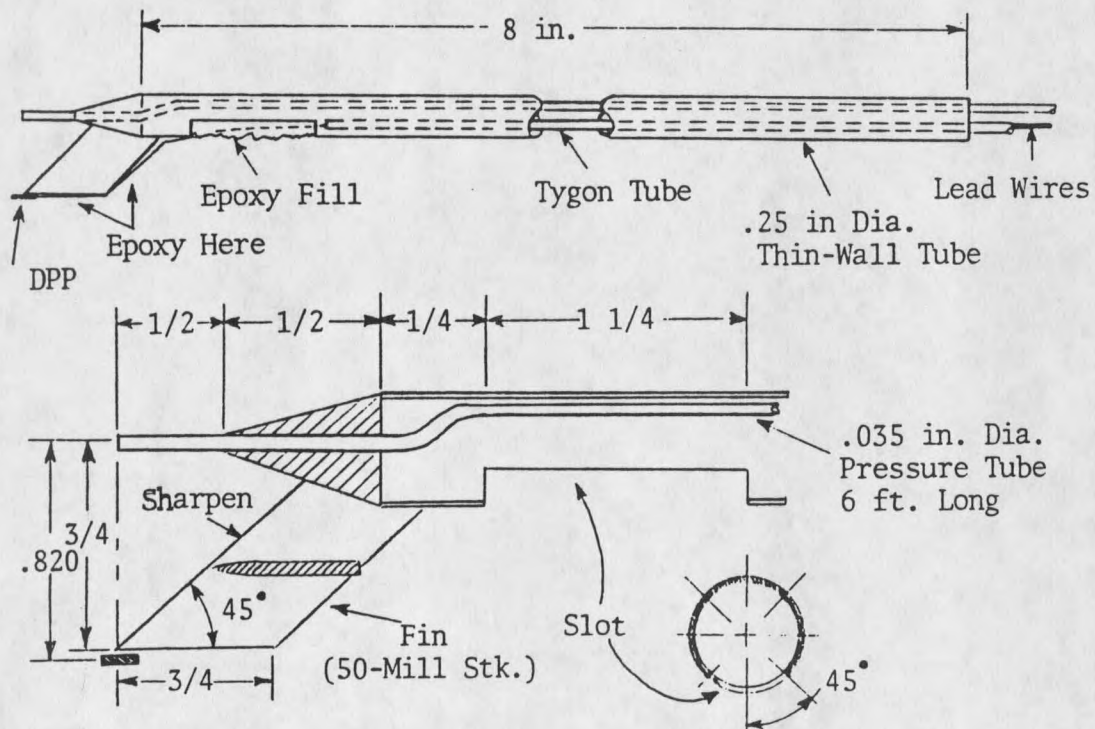


Figure 2. Major Features of the DPP.

The DPP measures pitot pressure fluctuations. What was required for this experiment was the velocity fluctuation. Therefore a relationship between pitot pressure fluctuation and velocity fluctuation is needed. Since the Mach number for this experiment was always greater than 1 the Rayleigh Supersonic Pitot Formula from [11] was used:

$$(1) \quad \frac{P}{P_P} = \left(\frac{2\gamma}{\gamma+1} M^2 - \frac{\gamma-1}{\gamma+1} \right)^{\frac{1}{\gamma-1}} / \left(\frac{\gamma+1}{2} M^2 \right)^{\frac{\gamma}{\gamma-1}}$$

Differentiating (1) yields

$$(2) \quad \frac{dP_P}{P_P} = \frac{dP}{P} + 2\gamma \left(\frac{2M^2 - 1}{2\gamma M^2 - (\gamma - 1)} \right) \frac{dM}{M}$$

Using the Mach number relation

$$(3) \quad \frac{dM}{M} = \frac{du}{u} - \frac{1}{2} \frac{dT}{T}$$

and the energy equation [11] with the assumption that $dT_0/T_0 = 0$,

$$(4) \quad \frac{dT}{T} = -(\gamma - 1)M^2 \frac{du}{u},$$

yields

$$(5) \quad \frac{dP_P}{P_P} = \frac{dP}{P} + \left[\gamma M^2 - \frac{(M^2 - 1)^2}{\left(M^2 - \frac{\gamma-1}{2\gamma} \right)} \right] \frac{du}{u}$$

Defining the term in brackets as the sensitivity s gives

$$(6) \quad \frac{dP_P}{P_P} = \frac{dP}{P} + s \frac{du}{u}$$

If the assumption that the pressure fluctuations inside of a boundary layer are much smaller than the velocity fluctuations is combined with the fact that the sensitivity is larger than 1 for $M > 1$, then the dP/P term can be eliminated giving

$$(7) \quad \frac{dP_P}{P_P} = s \frac{du}{u}$$

With (7) the DPP can now be used to determine velocity fluctuations, provided that the local Mach number is known.

Data Acquisition Systems

Three different acquisition systems were employed for the fluctuating measurements. The first system involved taking only wide band (sum of all frequencies) root mean square (RMS) voltage measurements. The second system involved taking data for power spectrum (frequency dependent RMS levels) measurements. The third system was used for taking intermittency (defined later) measurements. The equipment common to all three systems will be described first with the equipment distinct to each system described separately.

The DPP was connected to an electronic circuit, seen in Figure 3, which was connected to a Hewlett Packard 6202B d.c. power supply. This circuit was installed to eliminate any possibility of voltage spikes from the power supply affecting the DPP. The circuit also took the voltage from the power supply and reduced it by approximately one-third. This voltage level powered the DPP. The power supply was set at approximately 12–15 volts. Therefore, the DPP was supplied with 4–5 volts.

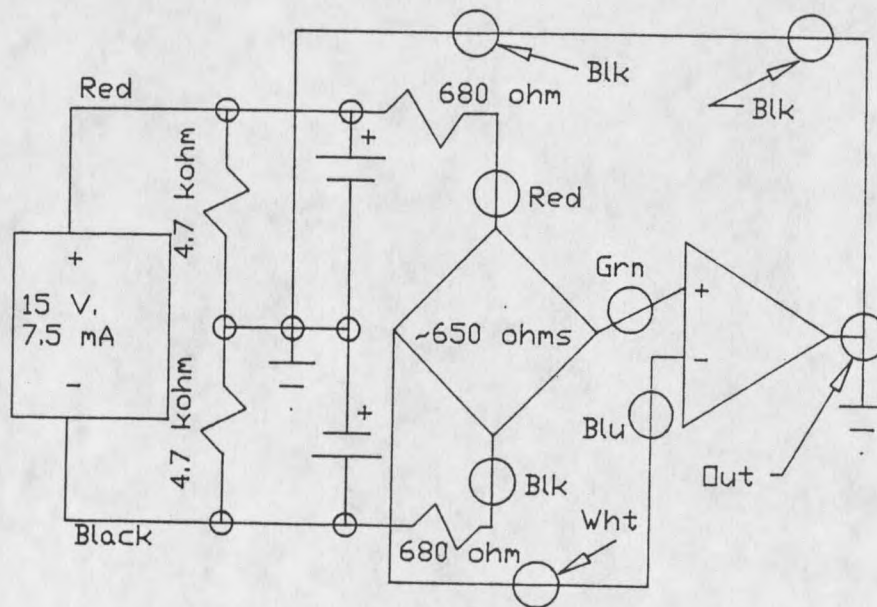


Figure 3. Electronic Circuit used with DPP.

